

A Discrete Cohesive Model for Fractal Cracks*

Michael P. Wnuk[†] Arash Yavari[‡]

3 December 2008

Abstract

The fractal crack model described here incorporates the essential features of the fractal view of fracture, the basic concepts of the LEFM model, the concepts contained within the Barenblatt-Dugdale cohesive crack model and the quantized (discrete or finite) fracture mechanics assumptions proposed by [Pugno and Ruoff \[2004\]](#) and extended by [Wnuk and Yavari \[2008\]](#). The well-known entities such as the stress intensity factor and the Barenblatt cohesion modulus, which is a measure of material toughness, have been re-defined to accommodate the fractal view of fracture.

For very small cracks or as the degree of fractality increases, the characteristic length constant, related to the size of the cohesive zone is shown to substantially increase compared to the conventional solutions obtained from the cohesive crack model. In order to understand fracture occurring in real materials, whether brittle or ductile, it seems necessary to account for the enhancement of fracture energy, and therefore of material toughness, due to fractal and discrete nature of crack growth. These two features of any real material appear to be inherent defense mechanisms provided by Nature.

Keywords: Fractal fracture, fractal crack, discrete fracture, cohesive model.

Contents

1	Introduction	1
2	Preliminaries: The Classic Cohesive Crack Model	3
3	Discretization of the Cohesive Crack Model	4
4	Discrete Cohesive Model for Fractal Cracks	7
5	Concluding Remarks	11

1 Introduction

The concept of discrete nature of fracture has been investigated by many researchers, beginning with [Neuber \[1958\]](#), [Novozhilov \[1969\]](#), [Wnuk \[1974\]](#), [Seweryn \[1994\]](#) and [Pugno and Ruoff \[2004\]](#). Comparison of various fracture criteria used to describe discrete fracture processes suggests that a certain finite length parameter, determined either by the microstructural or atomistic considerations, must be introduced into the basic equations underlying the theory of fracture. Even though various names and symbols have been used in describing this entity, such as “Neuber particle” by [Williams \[1957, 1965\]](#), “unit growth step” by [Wnuk \[1974\]](#) and “fracture quantum” by [Novozhilov \[1969\]](#) and [Pugno and Ruoff \[2004\]](#), the physical meaning of these length parameters is the same, and it can be accounted for mathematically by a discretization technique, cf. [Wnuk and Yavari \[2008\]](#) and [Pugno and Ruoff \[2004\]](#). See also [Taylor, et al. \[2005\]](#) and [Taylor \[2008\]](#).

*To appear in *Engineering Fracture Mechanics*.

[†]College of Engineering and Applied Science, University of Wisconsin - Milwaukee, Wisconsin 53201.

[‡]School of Civil and Environmental Engineering, Georgia Institute of Technology, Atlanta, GA 30332. E-mail: arash.yavari@ce.gatech.edu.

Remarkable success of Discrete Fracture Mechanics in modeling fracture caused by small-size cracks has prompted the present investigation. It is worth mentioning that discrete nature of fracture has been documented by numerous authors, above all by [Kfoury \[2008\]](#), [Taylor \[2008\]](#), [Ippolito, et al. \[2006\]](#) and many other investigators. The primary objective of the present research is to incorporate the concepts of fractal geometry and discrete nature of fracture propagation process into the cohesive crack model of [Barenblatt \[1962\]](#) and [Dugdale \[1960\]](#).

Cohesive models of fracture have been remarkably successful in explaining certain essential features of fracture processes such as a finite stress at the crack tip, a non-zero crack opening displacement at the tip of the crack, and a certain equilibrium length of the cohesive zone. This length increases with the applied load up to the point of incipient fracture and it serves as a measure of the material resistance to crack propagation. Mathematical elegance and simplicity of the cohesive crack model has stirred a large volume of research culminating with the work of [Carpinteri, et al. \[2002\]](#) and [Yavari \[2002\]](#). In [\[Carpinteri, et al., 2002\]](#) the authors used fractal concepts in building a fractal cohesive model to explain the experimentally observed size dependency of cohesive stress-strain curves in concrete. On the other hand, [Yavari \[2002\]](#) used similar concepts to show the equivalence of a fractal cohesive model with the fractal Griffith's models [\[Borodich, 1992, 1997\]](#).

In the present work we attempt to mathematically represent the discrete nature of fracture combined with its cohesive and fractal aspects. Barenblatt-Dugdale law of decohesion can be deduced from the present theory as a special case. Practical implications of the basic assumption of the model, i.e. the existence of the cohesive zone, have been pointed out in the research of [Pichler and Dormieux \[2007\]](#) as well as in many other investigations. [Pichler and Dormieux \[2007\]](#) demonstrated how the size of the cohesive zone determines the stress relaxation effect and Broberg's effect of energy screening which results in shielding of the crack tip by an energy dissipation mechanism. The larger is the equilibrium size of the cohesive zone, the more pronounced is the material ability to relax stresses prior to the onset of catastrophic fracture. In what follows we are going to show that discreteness of the fracture process and the fractal geometry both contribute to the enhancement of the equilibrium length of the cohesive zone associated with any given crack. It appears that these two attributes of fracture, discreteness and fractality, are used by Nature to shield a material from breaking up. Such features become particularly visible at nano-scale of the decohesion process.

We should mention that we have not been able to find any experimental results in the literature on the evolution of cohesive zone size during a quasi-static crack propagation. As [Das \[2003\]](#) also mentions "the behavior of the cohesive zone size as the crack extends, still remains the subject of research today." We believe that the present study can motivate future experimental works on the evolution of cohesive zone size.

A discretization procedure for the cohesive model of a fractal crack requires that all pertinent entities describing the influence of the cohesive stress that restrains opening of the crack, such as effective stress intensity factor, the modulus of cohesion, extent of the end zone and the opening displacement within the high-strain region adjacent to the crack tip are re-visited and replaced by certain averages over a finite length referred to as either "unit growth step", cf. [Wnuk \[1974\]](#) or "fracture quantum", cf. [Novozhilov \[1969\]](#) and [Pugno and Ruoff \[2004\]](#). Thus, two novel aspects of the model enter the theory: (1) degree of fractality related to the roughness of the newly created surface, and (2) discrete nature of the propagating crack. Both variables are shown to increase the effective fracture toughness. For previous works on cohesive fracture theories for fractal cracks see [Yavari \[2002\]](#) and [Wnuk and Yavari \[2003\]](#).

In this paper, three representations of fracture, namely (i) cohesive models, (ii) fractal models, and (iii) discrete models, are combined into one theory in order to better model a crack that can potentially be small and have rough surfaces. We shall begin with re-visiting this model and then go on to incorporate fractal and discrete nature of fracture occurring in real materials. Recent research on small cracks, cf. [Isupov and Mikhailov \[1998\]](#) and [Ippolito, et al. \[2006\]](#), indicate that the classic failure criteria break down for very small cracks. Such examples show the need for novel non-local failure criteria for design of structures, in which multiscale fracture mechanisms are present. In order to refine available mathematical tools and to extend their validity for nano-scale and for fractal (rough) cracks we will merge here the basic concepts of the cohesive crack model with the fractal view of the decohesion process. At the same time we shall employ the non-local criteria, which remain valid at atomistic or nano-scale levels.

In what follows we shall solve the problem assuming that we are dealing with a fractal crack represented by a cohesive model and that propagation of fracture is not continuous but discrete. Naturally, when the problem is reduced to that of a smooth crack and when the discrete nature of decohesion act is neglected the present model recovers the results identical to those known in classical fracture mechanics. The well-known entities such as

the stress intensity factor and the Barenblatt cohesion modulus, which is a measure of material toughness, have been re-defined to accommodate the fractal view of fracture. Specifically, the cohesion modulus, in addition to its dependence on the distribution of the cohesion forces, is shown now to be a function of the “degree of fractality” reflected by the fractal dimension D , or by the roughness exponent H . It is also a function of the unit growth step, the so-called fracture quantum and depends on the form of the “decohesion law”. As expected, in the limit of the fractal dimension D approaching 1 and for the disappearing magnitude of the fracture quantum, one recovers the cohesive crack model known from the fracture mechanics of smooth cracks.

This paper is structured as follows. In §2, the basic ideas of classical cohesive models are discussed. In §3, we introduce a discretization process for cohesive models. §4 presents a discrete cohesive model for fractal cracks. Conclusions are given in §5.

2 Preliminaries: The Classic Cohesive Crack Model

When a cohesive model is designed, the length of the physical crack c is extended by adding cohesive zones at both ends of the crack. Within these zones the restraining stress S counteracts the separation process. If the length of each cohesive zone is \tilde{R} , then the half-length of the extended crack becomes $a = c + \tilde{R}$ ¹. In order to solve the pertinent mixed boundary-value problem one needs to assume the following distribution of pressure applied along the surfaces of the extended crack

$$p(x) = \begin{cases} \sigma & 0 \leq |x| \leq c, \\ \sigma - S & c \leq |x| \leq a. \end{cases} \quad (2.1)$$

This is later superposed with the uniform tension $p(x) = -\sigma$ thus generating a stress-free crack with two cohesive zones, in which the S -stress is present, see Fig. 2.1. The second boundary condition is expressed in terms of the displacement component u_y , which is set equal zero along the symmetry axis outside the crack for $|x| \geq a$. The resulting solution is the familiar stress field, which in the vicinity of the crack tip contains the dominant term controlled by the stress intensity factor. This is the singular term that will be subject to annihilation. Such requirement of disappearance of the singular term is known as the “finiteness condition”. Note that S is, in general, a function of x , but here, for the sake of simplicity, we assume that S is constant.

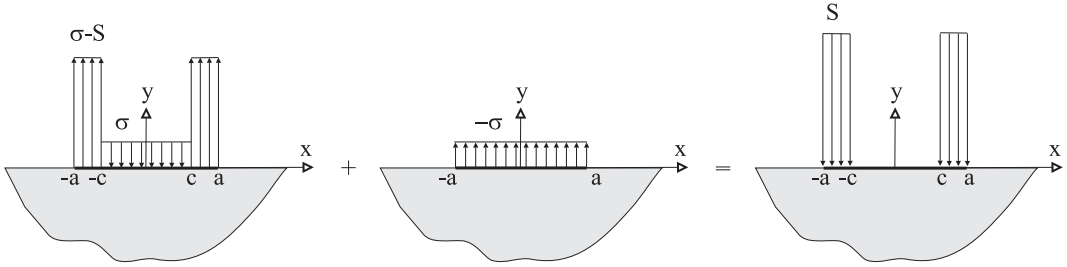


Figure 2.1: A cohesive crack and the associated pressure applied to the surface of the extended crack.

Before we can proceed to set up a finiteness condition for the crack pictured in Fig. 2.1, we need to evaluate K -factors associated with stresses σ and S . Applying the well-known LEFM expression

$$K_I = 2\sqrt{\frac{a}{\pi}} \int_0^a \frac{p(x)dx}{\sqrt{a^2 - x^2}} \quad (2.2)$$

we substitute (2.1) for the pressure $p(x)$ to obtain the stress intensity factor describing a cohesive crack

$$K_{\text{total}} = 2\sqrt{\frac{a}{\pi}} \left\{ \int_0^c \frac{\sigma dx}{\sqrt{a^2 - x^2}} + \int_c^a \frac{(\sigma - S)dx}{\sqrt{a^2 - x^2}} \right\} = 2\sqrt{\frac{a}{\pi}} \int_0^a \frac{\sigma dx}{\sqrt{a^2 - x^2}} - 2\sqrt{\frac{a}{\pi}} \int_c^a \frac{S dx}{\sqrt{a^2 - x^2}}. \quad (2.3)$$

¹Note that $\tilde{R} \leq c$.

It is seen that both σ and S contribute to the total stress intensity factor. Using the notation

$$K_\sigma = 2\sqrt{\frac{a}{\pi}} \int_0^a \frac{\sigma dx}{\sqrt{a^2 - x^2}} \quad \text{and} \quad K_S = 2\sqrt{\frac{a}{\pi}} \int_c^a \frac{S dx}{\sqrt{a^2 - x^2}} \quad (2.4)$$

we can rewrite equation (2.3) as

$$K_{\text{total}} = K_\sigma - K_S. \quad (2.5)$$

With constant σ and S the two K -factors are simplified to read

$$K_\sigma = \sigma \sqrt{\pi(c + \tilde{R})} \quad \text{and} \quad K_S = S \sqrt{\pi(c + \tilde{R})} \left[\frac{2}{\pi} \cos^{-1} \left(\frac{c}{c + \tilde{R}} \right) \right]. \quad (2.6)$$

These two stress intensity factors remain in equilibrium $K_\sigma = K_S$ during the process of loading up to the point of incipient fracture. The function K_σ^2 can be thought of as a “driving force”, which forces the crack to open up, while K_S^2 represents material resistance. It is noted that K_S reduces to zero for a vanishing length of the cohesive zone. For the physically important case of \tilde{R} being small compared to the crack length c , i.e., $\tilde{R} \ll c$, the second equation in (2.6) assumes the following simple asymptotic form.

$$K_S \sim \sqrt{\frac{2}{\pi}} \int_0^{\tilde{R}} \frac{S d\lambda}{\sqrt{\lambda}} = \sqrt{\frac{2}{\pi}} S (2\sqrt{\tilde{R}}). \quad (2.7)$$

The variable λ represents the distance measured backwards from the outer edge of the cohesive zone. In this limiting case the cohesion modulus does not depend on the crack size; it is expressed only in terms of the magnitude of the cohesive stress and the length \tilde{R} . Equating expression (2.7) with fracture toughness K_c and inverting the equation produces the ubiquitous result

$$\tilde{R} = \tilde{R}_c = \frac{\pi K_c^2}{8 S^2}. \quad (2.8)$$

This formula defines the characteristic length parameter as determined through the cohesive model of fracture. Three essential variables are related via this simple equation, which is valid only when $\tilde{R} \ll c$. Otherwise, equation (2.6) must be used to define the length of the cohesive zone as a function of the stresses σ , S and the crack size c .

Next, we employ the finiteness condition, which with (2.6) reads

$$\frac{\sigma\pi}{2} - S \cos^{-1} \left(\frac{c}{c + \tilde{R}} \right) = 0. \quad (2.9)$$

With $Q_D = \frac{\pi\sigma}{2S}$ one can solve equation (2.9) for the length of the cohesive zone to obtain

$$\frac{\tilde{R}}{c} = \sec Q_D - 1, \quad (2.10)$$

where $\sec = 1/\cos$. For small Q_D the right hand side reduces to $\frac{1}{2}Q_D^2$ and hence (2.10) reduces then to (2.8).

3 Discretization of the Cohesive Crack Model

In order to account for the discrete nature of the fracture processes all the K -factors discussed above need to be replaced by their averages. Applying the scheme [Pugno and Ruoff, 2004; Wnuk and Yavari, 2008]

$$K_\sigma \rightarrow \langle K_\sigma \rangle_{c,c+a_0} = \left(\frac{1}{a_0} \int_c^{c+a_0} K_\sigma^2 dc \right)^{\frac{1}{2}}, \quad K_S \rightarrow \langle K_S \rangle_{c,c+a_0} = \left(\frac{1}{a_0} \int_c^{c+a_0} K_S^2 dc \right)^{\frac{1}{2}} \quad (3.1)$$

we proceed to evaluate the averages defined in (3.1). The symbol a_0 denotes the fracture quantum, which is used as a normalization constant for the length-like variables X and R

$$X = \frac{c}{a_0}, \quad R = \frac{\tilde{R}}{a_0}. \quad (3.2)$$

The results are

$$\langle K_\sigma \rangle_{c,c+a_0} = \sigma\sqrt{\pi} \left(\frac{1}{a_0} \int_c^{c+a_0} (\xi + \tilde{R}) d\xi \right)^{\frac{1}{2}} = \sigma\sqrt{\pi a_0} \left(X + R + \frac{1}{2} \right)^{\frac{1}{2}}. \quad (3.3)$$

And

$$\langle K_S \rangle_{c,c+a_0} = S\sqrt{\pi} \frac{2}{\pi} \left\{ \frac{1}{a_0} \int_c^{c+a_0} (\xi + \tilde{R}) \left[\cos^{-1} \left(\frac{\xi}{\xi + \tilde{R}} \right) \right]^2 d\xi \right\}^{\frac{1}{2}} = (S\sqrt{\pi a_0}) \frac{2}{\pi} I(X, R)^{\frac{1}{2}}, \quad (3.4)$$

where

$$I(X, R) = \int_X^{X+1} (Y + R) \left[\cos^{-1} \left(\frac{Y}{Y + R} \right) \right]^2 dY. \quad (3.5)$$

Substituting (3.3) and (3.4) into the finiteness equation $\langle K_\sigma \rangle = \langle K_S \rangle$ yields

$$\frac{\sigma\pi}{2S} \left(X + R + \frac{1}{2} \right)^{\frac{1}{2}} = I(X, R)^{\frac{1}{2}}. \quad (3.6)$$

One can readily solve this equation for the loading parameter $Q = \sigma\pi/2S$ as a function of X and R . To distinguish this solution from the classic Dugdale solution (2.10) we shall use the subscript D for ‘‘Dugdale’’ and another subscript d for ‘‘discrete’’. From (3.6) it follows that

$$Q_{Dd} = \frac{I(X, R)^{\frac{1}{2}}}{\sqrt{X + R + \frac{1}{2}}}. \quad (3.7)$$

An interesting simplification of equation (3.7) is obtained for the limiting case of small ratios R/X or $\tilde{R}/c \ll 1$, i.e. LEFM. For this case the integral (3.5) reduces asymptotically to $2R$ because

$$I(X, R) = \int_X^{X+1} Y \left(1 + \frac{R}{Y} \right) \left[\cos^{-1} \left(\frac{1}{1 + R/Y} \right) \right]^2 dY. \quad (3.8)$$

But we know that

$$\left(1 + \frac{R}{Y} \right) \left[\cos^{-1} \left(\frac{1}{1 + R/Y} \right) \right]^2 = 2\frac{R}{Y} + O\left(\frac{R^2}{Y^2}\right), \quad (3.9)$$

where $O(\cdot)$ is Landau’s order symbol [Murray, 1984]. Thus

$$I(X, R) = 2R + \int_X^{X+1} O\left(\frac{R^2}{Y^2}\right) Y dY = 2R + O\left(\int_X^{X+1} \frac{R^2}{Y} dY\right) = 2R + O(R^2). \quad (3.10)$$

Therefore for $R \ll X$, equation (3.7) can be re-written as follows

$$Q_{Dd} \Big|_{R \ll X} = \sqrt{\frac{2R}{X + \frac{1}{2}}}. \quad (3.11)$$

The inverse relationship can be readily provided

$$R_{Dd} \Big|_{X \gg R} = \frac{(1 + 2X)Q_{Dd}^2}{4}. \quad (3.12)$$

Remark. As can be seen even for a vanishing crack length there exists a ‘‘residual’’ cohesive zone with the following finite length

$$\tilde{R}_{Dd}^{\text{inherent}} = \tilde{R}_{Dd}(X = 0) = \frac{a_0 Q_{Dd}^2}{4}. \quad (3.13)$$

When this quantity, labelled here as the ‘‘inherent cohesive zone’’ is set equal to the expression (2.8), one readily obtains the inherent strength for a flawless material σ_0 , namely

$$\sigma_0 = \sqrt{\frac{2}{\pi a_0}} K_c. \quad (3.14)$$

This interesting result is in complete agreement with the formula derived from the finite fracture mechanics, cf. [Pugno and Ruoff \[2004\]](#). When the inherent strength σ_0 is used as a normalization constant, then the stress at the onset of fracture due to a cohesive discrete crack subject to the condition $R \ll X$ can be expressed by a remarkably simple formula

$$\frac{\sigma_{Dd}^{\text{crit}}}{\sigma_0} = \frac{1}{\sqrt{2X+1}}. \quad (3.15)$$

This, again, is identical to the finite fracture mechanics result [[Taylor, et al., 2005](#); [Pugno and Ruoff, 2004](#)], and it should be compared to the Griffith (LEFM) result

$$\frac{\sigma_{\text{Griffith}}}{\sigma_0} = \frac{1}{\sqrt{2X}}. \quad (3.16)$$

Equation (3.15) resulted from setting the length R_{Dd} given by (3.12) equal to the critical value defined in (2.8).

The other interesting result is obtained for the asymptotic case of $X \gg 1$, i.e., for the situation when the fracture quantum a_0 vanishes. In this case the equation (3.7) reduces to a form identical with the Dugdale result, see equation (2.10). For $X \gg 1$ and arbitrary R we obtain

$$Q_{Dd} \Big|_{X \gg 1} \sim Q_D = \cos^{-1} \left(\frac{X}{X+R} \right). \quad (3.17)$$

The proof is as follows. Note that from the mean-value theorem we have

$$I(X, R) = (\bar{X} + R) \left[\cos^{-1} \left(\frac{\bar{X}}{\bar{X} + R} \right) \right]^2 \quad (3.18)$$

for some $\bar{X} \in (X, X+1)$. Note also that for large X , $\bar{X} \sim X$. Thus

$$Q_{Dd} = \frac{I(X, R)^{\frac{1}{2}}}{\sqrt{X+R+\frac{1}{2}}} = \sqrt{\frac{\bar{X}+R}{X+R+\frac{1}{2}}} \cos^{-1} \left(\frac{\bar{X}}{\bar{X}+R} \right) \sim \cos^{-1} \left(\frac{X}{X+R} \right) \quad \text{as } X \rightarrow \infty. \quad (3.19)$$

The inverse relation also agrees with equation (2.10). It is therefore justified to conclude that the results given for a discrete model of cohesive crack reduce to the known equations valid when discretization is removed. This is done by letting the fracture quantum approach zero and thus considering the limit $X \rightarrow \infty$. [Fig. 3.1](#) illustrates the differences and similarities between the solutions obtained from the discrete cohesive crack model and the classic Dugdale model. Examination of the graphs shown in [Fig. 3.1](#) reveals that for a given external dimensionless load Q , the nondimensional length of the cohesive zone R (which remains in equilibrium with the applied load) is greater for the discrete model. Thus, the measure of the material resistance to crack initiation is enhanced when the discrete nature of fracture is taken into account. Naturally, the differences are more pronounced for small cracks when the initial crack length is comparable to the magnitude of the fracture quantum a_0 .

Let us now take a look at the cohesion modulus of the discrete cohesive crack. From (3.4) we have

$$K_{\text{coh}}^d = \langle K_S \rangle = \frac{2}{\pi} S \sqrt{\pi a_0} I(X, R)^{\frac{1}{2}}. \quad (3.20)$$

When the size of the cohesion zone is small compared to the crack length, the integral in the equation (3.20) reduces to $2\tilde{R}/a_0$. For this case we obtain a simplified expression for the cohesion modulus, namely

$$K_{\text{coh}}^d \Big|_{R \ll X} = \frac{2}{\pi} S \sqrt{\pi a_0} \sqrt{\frac{2\tilde{R}}{a_0}}. \quad (3.21)$$

This relation shows explicitly that the product $S\sqrt{\tilde{R}}$ determines the material resistance to crack propagation. The problem faced by the material engineers consists in finding the right proportion between S and \tilde{R} ; there

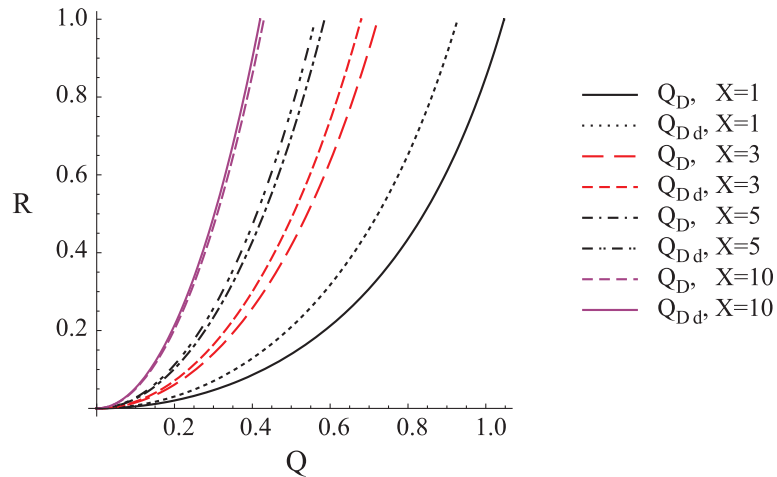


Figure 3.1: Length of the cohesive zone R as a function of the nondimensional load Q for two models: cohesive labelled by D and the discrete cohesive labelled by Dd .

exists a conflicting trend between the magnitude of the cohesive strength (approximated by the inherent strength of the material) and length of the cohesive zone. Increasing S , by increasing strength without paying attention to cohesion toughness parameter, which describes the degree of ductility, lowers the length \tilde{R} and thus it may lead to undesirable effects of increased brittleness. This is where the theoretical considerations involving the fracture quantum and the resulting discrete nature of fracture at small scales may prove useful in designing new materials. The formula (3.21) shows that indeed there is an additional length involved in defining the cohesion modulus; this is the length a_0 . As seen from (3.21), in addition to the inherent strength S , there are two other factors that influence material toughness; these are the fracture quantum and the ratio of cohesive zone size to fracture quantum. This provides a material engineer with additional degrees of freedom to work with. Yet another variable affecting the cohesion modulus and the material toughness is the roughness of the surfaces created in the course of fracture process. This will be discussed in the next section.

4 Discrete Cohesive Model for Fractal Cracks

It is known that fracture surfaces are rough and irregular and that cracks can be modelled by fractals. For the major theoretical results in fractal fracture mechanics see Mosolov [1991], Goldshtein and Mosolov [1991], Goldshtein and Mosolov [1992], Balankin [1997], Borodich [1997], Cherepanov, et al. [1995], Xie [1989], Xie and Sanderson [1995], Carpinteri [1994], Carpinteri and Chiaia [1996], Yavari, et al. [2000], Yavari, et al. [2002], Yavari [2002], Wnuk and Yavari [2003], Wnuk and Yavari [2005], Wnuk and Yavari [2008], and references therein.

In this section we shall incorporate two features typical of any fracture process:

- (1) Roughness of the newly created surfaces due to varying degree of fractality (as opposed to the assumption of perfectly smooth surfaces employed in the classical LEFM), and
- (2) Discrete nature of the separation of two adjacent surfaces caused by decohesion (as opposed to continuous character of the propagation process commonly assumed in all local fracture criteria).

We shall consider a fractal crack equipped with a cohesive zone. Therefore, we shall now be using all equations derived in the previous sections and modify them to fit the fractal model of Wnuk and Yavari [2003, 2005]. Although this model is only an approximation², it is the only model available at the present time.

The cohesive model assumes existence of two stress intensity factors, one associated with the applied stress, K_σ^f , and the other K_S^f assigned to the cohesive stress. Superscript “f” emphasizes the fact that we are dealing now with fractal cracks. When the discrete model is employed these two entities should be replaced by their

²The fractal crack model employed here is based on a simplifying assumption, according to which the original problem is approximated by considering a smooth crack embedded in the stress field generated by a fractal crack, cf. Wnuk and Yavari [2003].

averages taken over the interval $(c, c + a_0)$, where c denotes the half-nominal length of the crack and a_0 is the fracture quantum (see [Wnuk and Yavari \[2008\]](#)). For each value of the applied load one can determine the corresponding equilibrium length of the cohesive zone. Let us proceed with the calculations invoking the finiteness condition

$$\langle K_\sigma^f \rangle - \langle K_S^f \rangle = 0. \quad (4.1)$$

One needs to evaluate both terms in equation (4.1). Let us use a procedure similar to the one used in the previous section, in which we calculated the averages. Now we have the following scheme

$$\begin{aligned} K_\sigma &\rightarrow \langle K_\sigma^f \rangle_{c, c+a_0} = \left\{ \frac{1}{a_0} \int_c^{c+a_0} [K_\sigma^f(\xi, \tilde{R}, \alpha)]^2 d\xi \right\}^{\frac{1}{2}}, \\ K_S &\rightarrow \langle K_S^f \rangle_{c, c+a_0} = \left\{ \frac{1}{a_0} \int_c^{c+a_0} [K_S^f(\xi, \tilde{R}, \alpha)]^2 d\xi \right\}^{\frac{1}{2}}. \end{aligned} \quad (4.2)$$

The resulting functions depend on the fractal exponent α and the two dimensionless variables X and R . To calculate the K -factors for a fractal crack we employ the expression given by [Wnuk and Yavari \[2003\]](#) and obtain

$$K_I^f = \frac{a^{\alpha-1}}{\pi^{2\alpha-\frac{1}{2}}} \int_0^a \frac{(a-x)^{2\alpha} + (a+x)^{2\alpha}}{(a^2-x^2)^\alpha} p(x) dx. \quad (4.3)$$

In the first equation in (4.2) we substitute σ for $p(x)$ and $c + \tilde{R}$ for a . This leads to

$$K_\sigma^f(c, \tilde{R}, \alpha) = \chi(\alpha) \sigma \sqrt{\pi} (c + \tilde{R})^\alpha, \quad (4.4)$$

where

$$\chi(\alpha) = \frac{1}{\pi^{2\alpha}} \int_0^1 \frac{(1-s)^{2\alpha} + (1+s)^{2\alpha}}{(1-s^2)^\alpha} ds. \quad (4.5)$$

Next we evaluate the average

$$\langle K_\sigma^f \rangle = \chi(\alpha) \sigma \sqrt{\pi} \left\{ \frac{1}{a_0} \int_c^{c+a_0} (\xi + \tilde{R})^{2\alpha} d\xi \right\}^{\frac{1}{2}} = \chi(\alpha) \sigma \sqrt{\pi a_0^{2\alpha}} \left\{ \int_X^{X+1} (Y + R)^{2\alpha} dY \right\}^{\frac{1}{2}}. \quad (4.6)$$

This integral is simplified to read

$$\langle K_\sigma^f \rangle = \chi(\alpha) \sigma \sqrt{\pi a_0^{2\alpha}} \frac{[(X + R + 1)^{2\alpha+1} - (X + R)^{2\alpha+1}]^{\frac{1}{2}}}{\sqrt{2\alpha + 1}}. \quad (4.7)$$

Note that because $\alpha = \frac{2-D}{2}$, it is readily observed that for the fractal dimension $D = 1$ (or $\alpha = \frac{1}{2}$) expression (4.7) reduces to the non-fractal discretized cohesive model, i.e.

$$\langle K_\sigma \rangle = \sigma \sqrt{\pi a_0} \left(X + R + \frac{1}{2} \right)^{\frac{1}{2}}. \quad (4.8)$$

Let us define the ratio of the last two K -factors as

$$k_\sigma^f = \frac{\langle K_\sigma^f \rangle}{\langle K_\sigma \rangle} = a_0^{\alpha-\frac{1}{2}} \chi_\sigma(X, R, \alpha), \quad (4.9)$$

where

$$\chi_\sigma(X, R, \alpha) = \chi(\alpha) \left[\frac{(X + R + 1)^{2\alpha+1} - (X + R)^{2\alpha+1}}{(2\alpha + 1) (X + R + \frac{1}{2})} \right]^{\frac{1}{2}}. \quad (4.10)$$

The plot of the dimensionless function χ_σ versus α is shown in Fig. 4.1. Since χ_σ depends also on the crack length and the cohesive zone size, X and R , these two length-like variables are used as parameters in plotting

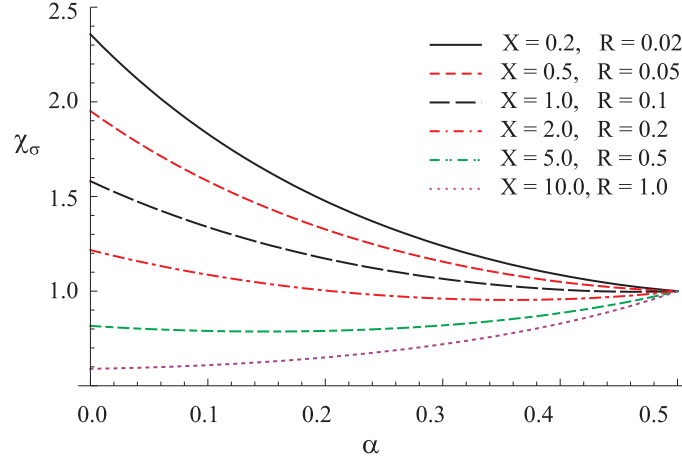


Figure 4.1: The function χ_σ versus α for different values of X and R .

the graphs in Fig. 4.1. The discrepancies in the χ_σ function are particularly visible for the fractal dimension D approaching 2 (or α approaching 0). This effect is reflected by the larger spread of function values at the vertical axis, where α equals zero.

For the other limiting case of α approaching $\frac{1}{2}$, when a fractal crack reduces to a smooth crack, all curves shown in Fig. 4.1 converge to unity, which means that the effects of fractal nature of the crack disappear and the solution for the discrete cohesive model is recovered. It can also be seen that for the crack sizes comparable to fracture quantum the magnitude of the average $\langle K_\sigma^f \rangle$ is enhanced for any α , while for cracks much longer than a_0 the value of this average tends to drop below the value $\langle K_\sigma \rangle$ valid for a smooth cohesive crack. Therefore, one may conclude that both the discrete nature of fracture and its fractal geometry alter the solutions obtained for the established cohesive crack models.

To further emphasize this point, we will evaluate and discuss the cohesion modulus as given by $\langle K_S^f \rangle$. This entity is a function of X , R and α , and its physical meaning is that of material resistance to initiation and propagation of rough cracks. Applying the second equation in (4.2) and substituting S for $p(x)$ in the integrand of (4.3), which is evaluated over the cohesive zone $c \leq x \leq a$, we obtain

$$\langle K_S^f \rangle = \frac{S}{\pi^{2\alpha - \frac{1}{2}}} \left\{ \frac{1}{a_0} \int_c^{c+a_0} (\xi + \tilde{R})^{2\alpha} \left[\int_{\frac{c}{c+\tilde{R}}}^1 \frac{(1-s)^{2\alpha} + (1+s)^{2\alpha}}{(1-s^2)^\alpha} ds \right]^2 d\xi \right\}^{\frac{1}{2}}. \quad (4.11)$$

Or, in terms of X and R

$$\langle K_S^f \rangle = S \sqrt{\pi a_0^{2\alpha}} \left\{ \int_X^{X+1} (Y+R)^{2\alpha} H^2(Y, R, \alpha) dY \right\}^{\frac{1}{2}}, \quad (4.12)$$

where

$$H(Y, R, \alpha) = \int_{\frac{Y}{Y+R}}^1 \frac{(1-s)^{2\alpha} + (1+s)^{2\alpha}}{\pi^{2\alpha} (1-s^2)^\alpha} ds. \quad (4.13)$$

Written in a somewhat shorter form the above expression reads

$$\langle K_S^f \rangle = S \sqrt{\pi a_0^{2\alpha}} G_{\text{coh}}^f(X, R, \alpha), \quad (4.14)$$

where

$$G_{\text{coh}}^f(X, R, \alpha) = \left[\int_X^{X+1} (Y+R)^{2\alpha} H^2(Y, R, \alpha) dY \right]^{\frac{1}{2}}. \quad (4.15)$$

We note that for $\alpha = \frac{1}{2}$ the function H reduces to

$$H\left(X, R, \frac{1}{2}\right) = \frac{2}{\pi} \cos^{-1}\left(\frac{c}{c + \bar{R}}\right) \quad (4.16)$$

and the function G_{coh}^f becomes identical with the non-fractal result obtained previously for a discrete cohesive crack, i.e.

$$G_{\text{coh}}^f\left(X, R, \frac{1}{2}\right) = \frac{2}{\pi} I^{\frac{1}{2}}(X, R). \quad (4.17)$$

The cohesion modulus for $\alpha = \frac{1}{2}$ acquires the form

$$\left\langle K_S^f \right\rangle \Big|_{\alpha=\frac{1}{2}} = (S\sqrt{\pi a_0}) \frac{2}{\pi} I^{\frac{1}{2}}(X, R) \quad (4.18)$$

as expected.

To better understand the effects of fractality and discrete aspects of fracture on the cohesion modulus let us examine the ratio

$$\chi_S = \frac{\left\langle K_S^f \right\rangle}{\left\langle K_S \right\rangle} = \frac{G_{\text{coh}}^f(X, R, \alpha)}{\frac{2}{\pi} I^{\frac{1}{2}}(X, R)}. \quad (4.19)$$

Fig. 4.2 provides the diagrams illustrating the dependence of this function on the fractal exponent α and the two length-like variables X and R . The best way to visualize the effect of these variables is to think of the ratio R/X . As seen from the graph in Fig. 4.2 the material toughness measured for fractal and discrete fracture, as given by expressions (4.14) and (4.19), can be either enhanced or reduced when the set of the independent variables (X, R, α) is manipulated. The range of $\chi_S > 1$ corresponds to an enhancement of the material resistance to crack initiation due to variations in the degree of fractality of the crack surfaces. The enhancement is seen to occur for the fractal dimension D approaching 2 and crack sizes small in comparison to the constant a_0 . The effect is pertinent to very small cracks.

Now we have all the entities needed to set up the finiteness condition. Recalling the equality $\langle K_\sigma^f \rangle = \langle K_S^f \rangle$ and using (4.2) and (4.14) we arrive at

$$\chi(\alpha)\sigma\sqrt{\pi a_0^{2\alpha}} \left[\frac{(X+R+1)^{2\alpha+1} - (X+R)^{2\alpha+1}}{2\alpha+1} \right]^{\frac{1}{2}} = S\sqrt{\pi a_0^{2\alpha}} G_{\text{coh}}^f(X, R, \alpha). \quad (4.20)$$

This can be solved explicitly for the loading parameter $Q_f = \pi\sigma_f/2S$ as a function of X, R and α (or implicitly for R as a function of Q, X and α). The solution is

$$Q_f = \frac{\pi}{2\chi(\alpha)} G_{\text{coh}}^f(X, R, \alpha) \left[\frac{2\alpha+1}{(X+R+1)^{2\alpha+1} - (X+R)^{2\alpha+1}} \right]^{\frac{1}{2}}. \quad (4.21)$$

What we would like to derive from this equation is the functional dependence of the nominal length of the cohesive zone R_f on the loading parameter Q_f (from now on the length R will be denoted by R_f to emphasize the fact that it pertains to a fractal crack). This can be done by inverting the function (4.21). The graphs of R_f versus Q_f are shown in Fig. 4.3. When the exponent α varies within the interval $[0, \frac{1}{2}]$ the curves in Fig. 4.3 pertain to fractal and discrete fracture. For each case shown the length of the cohesive zone at fixed applied load is demonstrated to increase with increasing the fractal dimension D . Such a result proves that fractal geometry of a crack and/or the discrete nature of fracture tends to increase the material resistance to crack initiation and propagation. It also shows that a fractal crack is capable of relaxing the high stress near the crack tip by generating a larger cohesive zone.

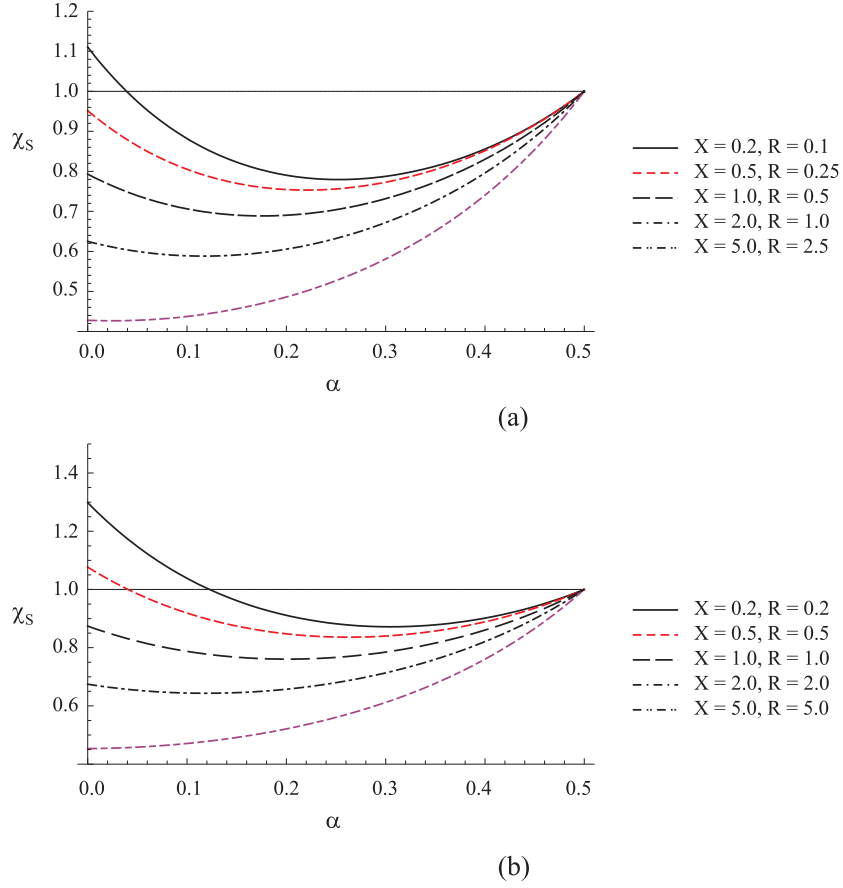


Figure 4.2: The function χ_S versus α for different values of X . (a) $R/X = 0.5$, (b) $R/X = 1.0$.

5 Concluding Remarks

Relations between applied load and the equilibrium length of the cohesive zone have been established for the following three different mathematical representations of a crack:

- (i) Cohesive crack model of Dugdale-Barenblatt for a smooth crack described by the two K -factors K_σ and K_S corresponding to the applied stress and the cohesive stress, respectively.
- (ii) Discrete cohesive crack model described by the averages $\langle K_\sigma \rangle_{c,c+a_0}$ and $\langle K_S \rangle_{c,c+a_0}$.
- (iii) Discrete and fractal cohesive crack model involving the fractal equivalents of the averages used in part (ii), namely $\langle K_\sigma^f \rangle_{c,c+a_0}$ and $\langle K_S^f \rangle_{c,c+a_0}$.

For a classic LEFM crack model there is no cohesive zone, and the crack itself provides a mechanism for relaxing the high stresses in the vicinity of a stress concentrator. Therefore, this representation may be thought of as a limiting case of a more general and refined mathematical formulation involving a cohesive zone associated with a crack. For such a representation the equilibrium between the driving force K_σ^2 and the material resistance K_S^2 defines a unique relation between the length of the cohesion zone, say \tilde{R} , and the applied load, say Q . The equilibrium between $R = \frac{\tilde{R}}{a_0}$ and Q is maintained during the loading process up to the point of incipient fracture.

The cohesive zone generated prior to fracture has two important aspects. It measures the material resistance to fracture. The longer is the cohesive zone, the greater is the resistance. It also provides a mechanism for relaxing stresses prior to fracture in the immediate vicinity of a stress concentrator.

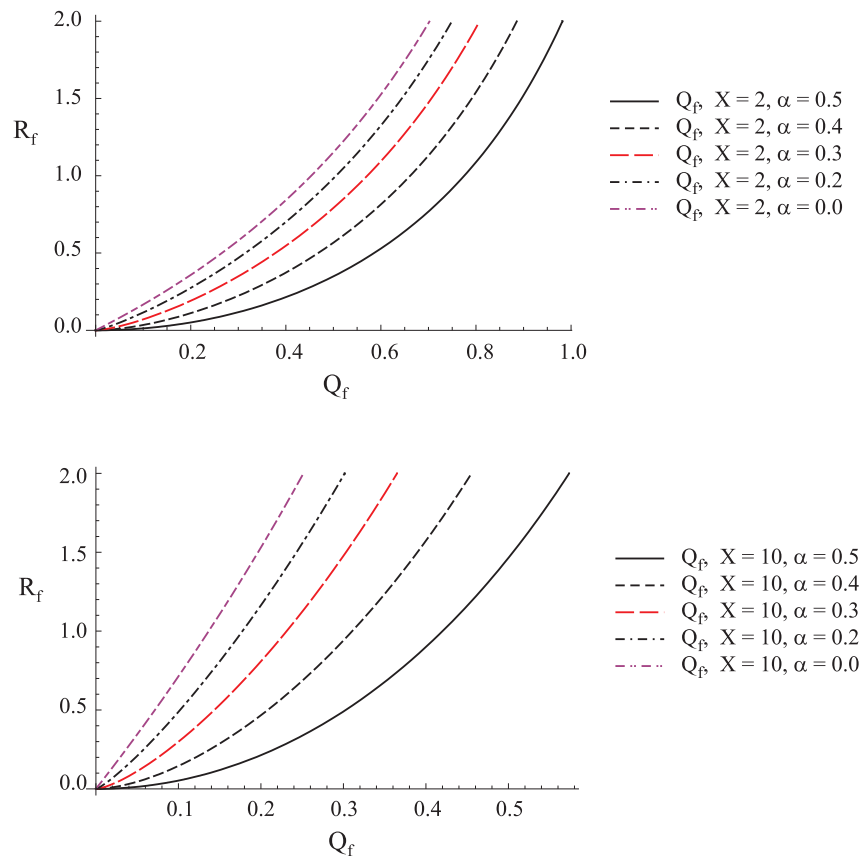


Figure 4.3: The function R_f versus Q_f for $X = 2$ and $X = 10$ and different values of α .

Fig. 5.1 schematically shows four sketches of a crack represented by four mathematical models: (a) the LEFM concept of a Griffith crack embedded in a linear elastic solid, (b) Dugdale-Barenblatt cohesive model, (c) discrete cohesive model, and finally, and (d) fractal discrete cohesive model. The very first crack shown in the figure has no cohesive zone at all, and the stresses are singular at the tip of the crack. In this case fracture toughness must be measured by employing the ASTM standards that make no mention of cohesion. The second crack in the figure corresponds to a cohesive model suggested independently by Dugdale [1960] and Barenblatt [1962]. With cohesion included we gain a better insight into the material response to fracture by visualizing the effect of the cohesive zone. As it turns out, it is a certain integral of the cohesion stress $S(x)$ over the zone R . For a constant S and under the restriction of $\frac{R}{X} \ll 1$ this integral reduces to a product of S and the square root of the length R . This is Barenblatt's cohesion modulus, which determines the material resistance to onset and propagation of fracture. Here, we have generalized this expression for a discrete fracture and with the fractal geometry taken into account. Thus, our model incorporates the discrete nature of fracture processes and its fractal geometry at the same time. Two new variables enter the theory: (1) fracture quantum a_0 , and (2) degree of fractality measured either by the fractal dimension D or by the fractal exponent α .

At the micro- and nano-scale the size of the *Neuber particle*, or *process zone* in a more updated nomenclature, becomes important not only for mathematical treatment of the problem, but also for the physical interpretation of the decohesion phenomenon at the atomistic scale. It is noteworthy that each of the successive models listed in Fig. 5.1 predicts for a given level of the applied load successively larger cohesive zones, namely

$$R_{Dd}^f \geq R_{Dd} \geq R_D \geq R_{LEFM} = 0. \quad (5.1)$$

The interpretation of the subscripts is as follows: f - fractal, Dd - Dugdale discrete, D - Dugdale. Of course, the LEFM value of R is zero, but using the K_c value obtained from the tests specified by ASTM one can, in a hindsight, define an equivalent length R that could be associated with a LEFM crack.

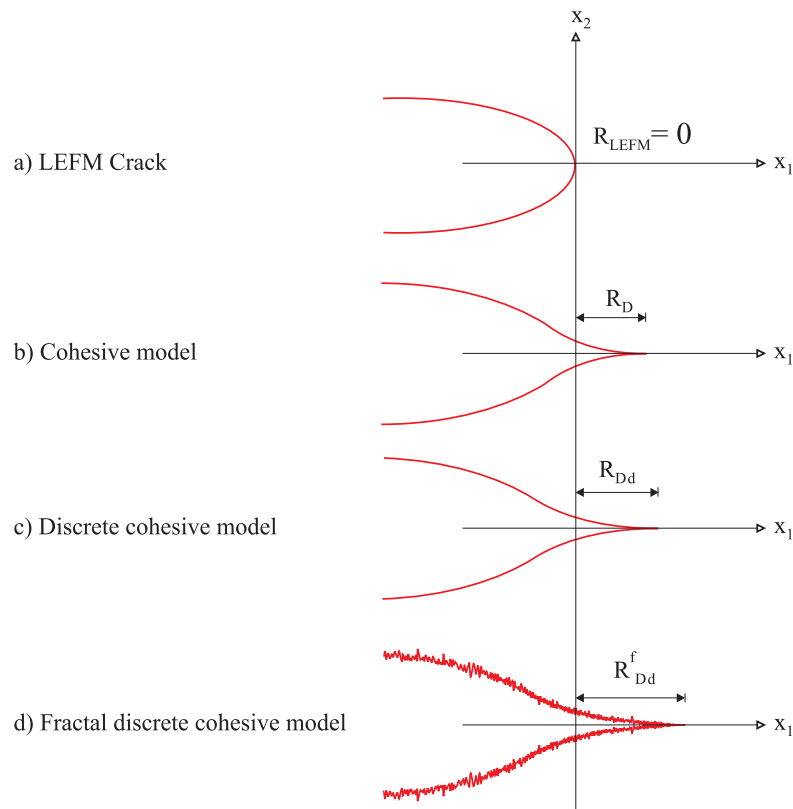


Figure 5.1: Discrete growth of a cohesive fractal crack and its auxiliary cohesive smooth crack.

References

- Balankin, A.S. (1997). Physics of fracture and mechanics of self-affine cracks. *Engineering Fracture Mechanics* **57**(2),135–203.
- Barenblatt, G. I. (1962) The mathematical theory of equilibrium of crack in brittle fracture. *Advances in Applied Mechanics* **7**:55-129.
- Borodich, F.M. (1992). Fracture energy in a fractal crack propagating in concrete or rock. *Doklady Akademii Nauk*, **325**, 113881141.
- Borodich, F.M. (1997). Some fractal models of fracture. *Journal of the Mechanics and Physics of Solids* **45**(2),239–259.
- Carpinteri, A. Scaling Laws and Renormalization-Groups for Strength and Toughness of Disordered Materials. *International Journal of Solids and Structures*, **31**:291-302, 1994.
- Carpinteri, A. and Chiaia, B. and Cornetti, P. [2002], A scale-invariant cohesive crack model for quasi-brittle materials. *Engineering Fracture Mechanics* **69**:207-217.
- Carpinteri, A. and Chiaia, B. Crack-resistance behavior as a consequence of self-similar fracture topologies. *International Journal of Fracture*, **76**:327-340, 1996.
- Cherepanov, G. P., Balankin, A.S., and Ivanova, V. S. (1995). Fractal fracture mechanics – A review. *Engineering Fracture Mechanics* **51**(6),997–1033.
- Das, S. [2003], Spontaneous complex earthquake rupture propagation. *Pure and Applied Geophysics* **160**:579-602.

- Dugdale, D. S. (1960) Yielding of Steel Sheets Containing Slits. *Journal of the Mechanics and Physics of Solids* **8**:100-104.
- Goldshtein, R.V. and Mosolov, A.A. (1991). Cracks with a fractal surface. *Soviet Physics Doklady* **38**(8),603–605.
- Goldshtein, R.V. and Mosolov, A.A. (1991). Fractal cracks. *Journal of Applied Mathematics and Mechanics* **56**(4),563–571.
- Ippolito, M. and Mattoni, A. and Colombo, L. and Pugno, N. (2006) Role of lattice discreteness on brittle fracture: Atomistic simulations versus analytical models. *Physical Review B* **73**:104111.
- Isupov, L. P. and Mikhailov, S. E. (1998) A comparative analysis of several nonlocal fracture criteria. *Archive of Applied Mechanics* **68**:597-612.
- Jin, Z. H. and Sun, C. T. [2006], A comparison of cohesive zone modeling and classical fracture mechanics based on near tip stress field. *International Journal of Solids and Structures* **43**:1047-1060.
- Kfourri, A. P. [2008], Characteristic crack-tip distances in fracture criteria: Is crack propagation discontinuous? *Engineering Fracture Mechanics* **75**:1815-1828.
- Mosolov, A.A. (1991). Cracks with fractal surfaces. *Dokl. Akad. Nauk SSSR* **319**(4),840–844.
- Murray, J.D. (1984), *Asymptotic Analysis*, Springer-Verlag, New York.
- Neuber, H. (1958), *Theory of Notch Stresses*, Springer-Verlag, Berlin.
- Novozhilov, V.V. (1969) On a necessary and sufficient criterion for brittle strength. *Journal of Applied Mathematics and Mechanics-USSR* **33**:212-222.
- Pichler, B. and Dormieux, L. [2007], Cohesive zone size of microcracks in brittle materials. *European Journal of Mechanics A-Solids* **26**:956-968.
- Pugno, N. and Ruoff, R. S. (2004). Quantized fracture mechanics. *Philosophical Magazine* **84**(27),2829–2845.
- Seweryn, A. (1994) Brittle-Fracture Criterion for Structures with Sharp Notches. *Engineering Fracture Mechanics*, **47**:673-681.
- Taylor, D. and Cornetti, P. and Pugno, N. (2005) The fracture mechanics of finite crack extension. *Engineering Fracture Mechanics*, **72**:1021-1038.
- Taylor, D. (2008) The theory of critical distances. *Engineering Fracture Mechanics*, **75**:1696-1705.
- Williams, M. L. (1957) On the stress distribution at the base of stationary cracks. *Journal of Applied Mechanics* **24**:109-114.
- Williams, M. L. (1965) Dealing with singularities in elastic mechanics of fracture. *11th Polish Symposium on Mechanics of Solids*, Krynica, Poland.
- Wnuk, M. P. (1974) Quasi-static extension of a tensile crack contained in a viscoelastic-plastic solid. *Journal of Applied Mechanics* **41**:234-242, 1974.
- Wnuk, M.P., and Yavari, A. (2003). On estimating stress intensity factors and modulus of cohesion for fractal cracks. *Engineering Fracture Mechanics* **70**,1659–1674.
- Wnuk, M. P. and Yavari, A. (2005) A correspondence principle for fractal and classical cracks. *Engineering Fracture Mechanics* **72**:2744-2757.
- Wnuk, M. P. and Yavari, A. (2008) Discrete fractal fracture mechanics. *Engineering Fracture Mechanics* **75**(5):1127-1142.

- Xie, H. (1989). The fractal effect of irregularity of crack branching on the fracture toughness of brittle materials. *International Journal of Fracture*, **41**,267–274.
- Xie, H. and Sanderson, D.J. (1995). Fractal effects of crack propagation on dynamic stress intensity factors and crack velocities. *International Journal of Fracture* **74**,29–42.
- Yavari, A., Hockett, K.G., and Sarkani, S. (2000). The fourth mode of fracture in fractal fracture mechanics. *International Journal of Fracture* **101**(4),365–384.
- Yavari, A. (2002) Generalization of Barenblatt's cohesive fracture theory for fractal cracks. *Fractals-Complex Geometry Patterns and Scaling in Nature and Society* **10**:189-198.
- Yavari, A., Sarkani, S., and Moyer, E.T. (2002). The mechanics of self-similar and self-affine fractal cracks. *International Journal of Fracture* **114**,1–27.